2018

# Pressure Drop Of Condensation From Superheated Vapor Inside Horizontal Smooth Round Tubes

Jiange Xiao
*ACRC, the University of Illinois*, jxiao10@illinois.edu

Predrag S. Hrnjak
pega@illinois.edu

# Pressure Drop Of Condensation From Superheated Vapor Inside Horizontal Smooth Round Tubes

Jiange XIAO[1], Pega HRNJAK[1,2]*

[1]University of Illinois at Urbana-Champaign, Department of Science and Engineering,

Urbana, IL, USA

Jxiao10@illinois.edu, pega@illinois.edu

[2]Creative Thermal Solutions,

Urbana, IL, USA

* Corresponding Author

## ABSTRACT

Pressure drop of R134a, R32 and R1233zd(E) is measured and reported in diabatic conditions during condensation from superheated vapor inside horizontal smooth round tubes. The test conditions include mass fluxes from 100 to 400 kg/m$^2$-s, heat fluxes from 5 to 15 kW/m$^2$ and tube diameters of 4.0 and 6.1 mm at saturation temperatures of 30 $^o$C. Compared to a conventional pressure drop model constructed under the assumption of thermal equilibrium, the experimental data clearly shows that the onset and end of condensation is changing instead of being fixed at bulk quality 1 and 0. This discrepancy between the theory and reality results in a deviation between the prediction and data, especially in the condensing superheated (CSH) region. The result shows an increase in pressure drop as mass flux increases. Tube size also affects the pressure drop in that smaller tube yields higher pressure drop. A further comparison between the different refrigerants conditions illustrates the effects of properties such as liquid-vapor density ratio, liquid viscosity, surface tension and latent heat. The results are analyzed along with the visualizations of the flow. While viscosity and velocity gradient determines the magnitude of pressure drop, the waves on the interface and the velocity of the bulk flow are identified as the two competing factors affecting pressure drop when condensation proceeds. The process as described in this paper provides an insight for a mechanistic model that traces the development of the flow to help resolve the issues in conventional "3-zone" pressure drop models.

## 1. INTRODUCTION

The condensation process in a condenser of a vapor-compression system is typically modeled as a "3-zone" model as in Fig. 1. The model assumes thermal equilibrium, meaning each element in the volume being evaluated shares the same temperature, pressure and fluid property. This assumption also leads to an inference that by knowing temperature,

pressure and quality, parameters such as void fraction, flow regime and flow velocity are determined. In a condenser, however, the assumption of thermal equilibrium does not hold due to the temperature gradient required by the heat transfer process. Because of the temperature gradient, as soon as the inner wall temperature drops to the saturation temperature, condensation starts even though the specific enthalpy still indicates superheated vapor. It goes the same for the end of condensation. Two more regions with two-phase flow are present in the condensation process as shown in Fig. 2 due to the non-equilibrium. Not taking the non-equilibrium into account could have profound impacts on the view of the condensation process. Take heat transfer coefficient (HTC) as an example, it has been measured and described by Kondo and Hrnjak (2011a, 2011b, 2012) and Agarwal and Hrnjak (2013) that HTC in the CSH region is much higher than that of single-phase heat transfer. The much higher HTC in the CSH region suggests a potential to reduce the size of the condenser in a vapor-compression system when the CSH region is comparable in size against the two-phase (TP) region. The existence of liquid in the CSH region is shown by Meyer and Hrnjak (2017) through the flow visualization and film thickness measurement of R134a. The effects of non-equilibrium on void fraction, flow regime and HTC are furthered by Xiao and Hrnjak (2016, 2017a, 2017b). Mechanistic models are purposed to predict the HTC throughout all five regions. The current studies still lack discussions on the pressure drop behavior with non-equilibrium effects considered. To elaborate on the subject, this paper presents the pressure drop data during condensation in a horizontal round tube from superheated vapor.

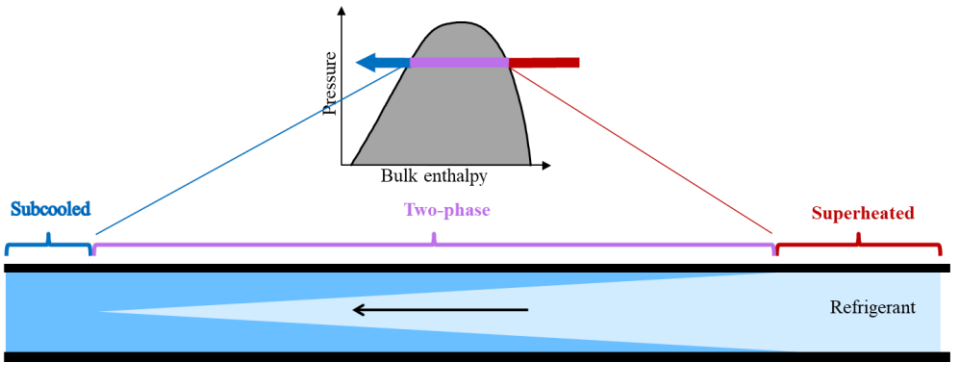


**Figure 1:** "3-zone" model of the condensation process

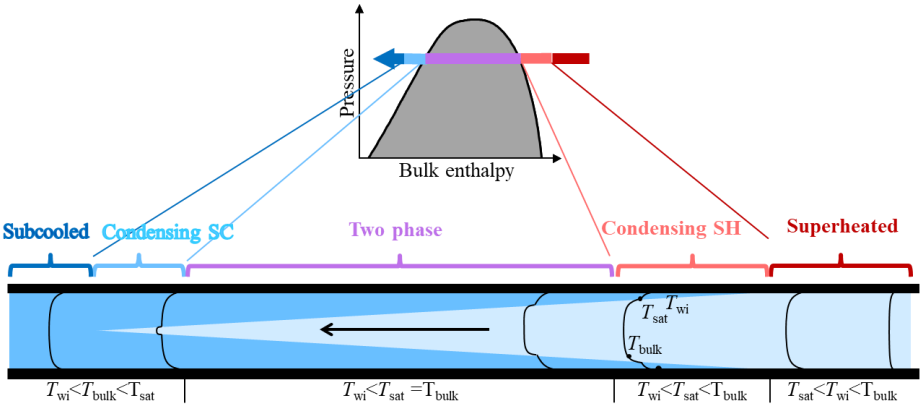


**Figure 2:** "5-zone" model of the condensation process.

## 2. EXPERIMENT DESCRIPTION

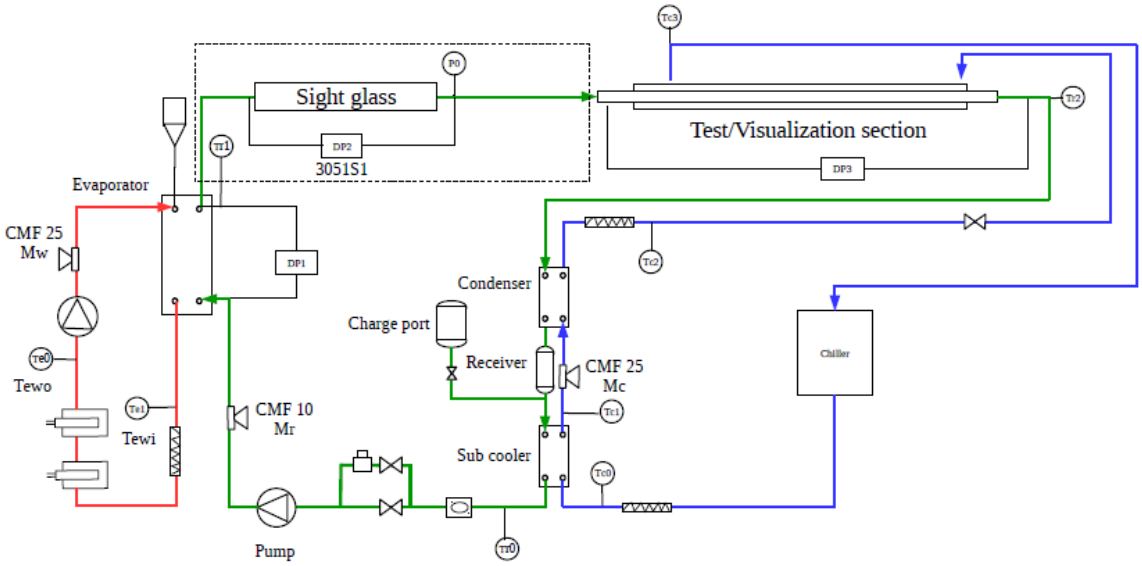


**Figure 3:** Schematic drawing of the facility

Fig. 3 presents the schematic drawing of the facility where the pressure drop is measured and visualizations are taken. The facility consists of the refrigerant, water and glycol loops. Subcooled refrigerant is pumped through the gear pump located at the bottom of the facility into the evaporator. Inside evaporator is water heated up by heaters. The mass flow rate of water is measured by the Coriolis flow meter. The inlet and outlet temperature of the water is measured by thermocouples calibrated to the accuracy of ±0.2 ºC. Through energy balance, the state of the refrigerant at the inlet of the test/visualization section is calculated. The test section is a 6.1 or 4.0 mm round copper tube inside a polycarbonate tube as a coaxial heat exchanger. Pressure drop is measured in the test section diabatically with differential pressure transducer to the accuracy of ±0.1% full-scale. When the copper tube is changed to a glass tube, the test section is made into a transparent visualization section. High-speed videos are taken at similar conditions as when pressure drop data is taken. The secondary fluid inside the polycarbonate tube is glycol. The inlet and outlet temperature as well as the mass flow rate of the glycol is measured for energy balance. The refrigerant is then subcooled by two plate heat exchangers serving as condenser and subcooler before entering the pump again.

## 3. RESULTS AND DISCUSSIONS

### 3.1 Effects of the mass flux

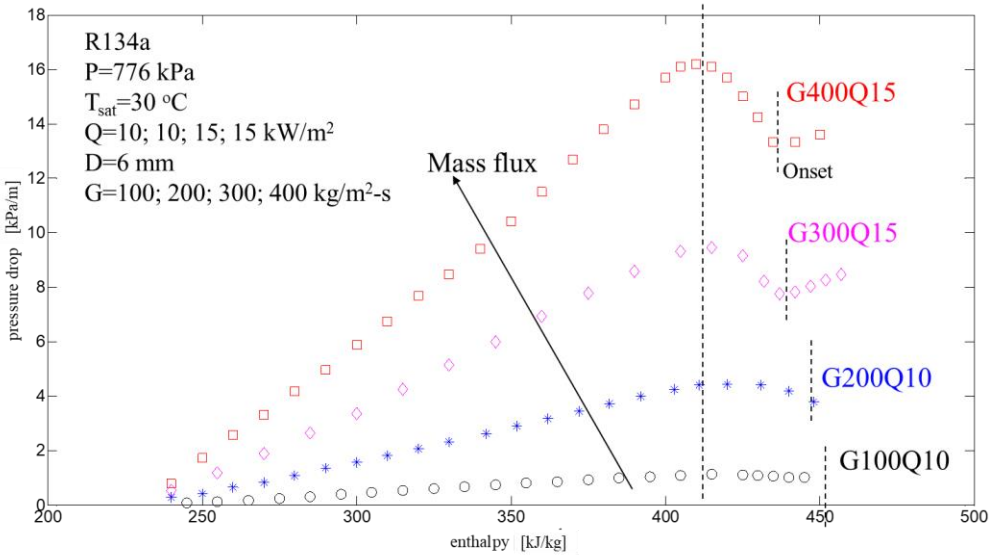


**Figure 4:** Pressure drop increases with mass flux.

From Fig. 4, when mass flux is increased, pressure drop increases. It is obvious because the velocity gradient of the refrigerant together with the viscosity determines the pressure drop. The higher the mass flux, the higher the velocity gradient. What is interesting in Fig. 4 is the pressure drop at specific enthalpy larger than that of the thermal dynamic (bulk) quality 1, where the refrigerant is superheated vapor in a "3-zone" model. If the refrigerant is superheated vapor, the pressure drop will consistently go down as the specific enthalpy decreases because the density increases and no other mechanisms kick in. It is indeed the case before the onset of condensation as suggested by the short dashed lines. However, after the onset of condensation as the wall temperature drops to lower than the saturation temperature, the pressure drop actually goes up rather than going down despite the increasing density. Fig. 5 provides an explanation of the pressure drop behavior in the CSH region. Even before the specific enthalpy drops below that of bulk quality 1, there are already waves inside the tube because of the condensation. Waves are the result of interaction between the faster-flowing core vapor and the liquid film dragged by the shear from vapor. Due to instabilities such as Kelvin-Helmholtz and Rayleigh-Taylor, the velocity and density differences between liquid and vapor generate waves that dissipate energy at the interface. The dissipation of energy is presented in the pressure drop. Therefore, even when the flow velocity decreases as the specific enthalpy decreases, the pressure drop still increases due to this dissipation. As the condensation proceeds, even though the wave is temporally larger due to higher liquid load, the flow velocity is dropping. Eventually the pressure drop decreases with decreasing specific enthalpy again because the dropping of flow velocity and slip velocity overshadows the increasing dissipation at the interface. At the early stages of condensation, the increasing waviness and decreasing flow velocity competes with each other and creates the peak of pressure drop somewhere around bulk quality 1 depending on the working conditions.

Another notion from Fig. 5 is the different flow regimes with different mass fluxes. At the entrance stages of condensation, the flow regime is always annular because the entire circumference of the tube is generating condensate. Meanwhile, the liquid film is not thick enough to be affected by the gravity and shear force. After the liquid film becomes thicker, the flow regime starts to change according to the balance between the gravity and shear force. When the mass flux is 100 kg/m$^2$-s, the gravitational force dominates over shear force. After the bulk quality drops to around 0.8 the bottom of the tube apparently holds more liquid than on the top. The flow regime is then changed from the annular to stratified-wavy. The transition happens because the surface tension is not enough to hold sufficient liquid film on the top and the shear force that carries the condensate downstream cannot mitigate the pulling from the gravity. When the mass flux is 400 kg/m$^2$-s, the annular flow persists until bulk quality is about 0.2. The transition is from annular to a mixing mode between stratified-wavy and intermittent flow. Unlike low mass fluxes like 100 kg/m$^2$-s, the shear force under 400 kg/m$^2$-s is much larger. It means even though the gravity is still pulling liquid down to the bottom, most condensate is dragged forward by the much faster vapor core downstream, making the liquid film very

uniform around the tube wall. Unlike stratified-wavy flow, where the waves grow mostly in the liquid pool, the waves grow much more uniformly in annular flow. As more liquid is generated, the waves first becomes stronger as indicated by the shades in Fig. 5 at G=400 kg/m$^2$-s. Then the waves start to collapse onto each other, forming larger waves. When the liquid load is large enough, the waves wash to the top of the tube, forming intermittent flow. At the same time, due to the pulling by gravity, the liquid film is much thicker at the bottom than the top. Thus the flow regime is both intermittent because the cross section of the tube is blocked by liquid slug, and stratified because the gravity pulls the condensate to the bottom. For the sake of simplicity, this type of flow is called intermittent flow in this paper. The mechanisms that affect the pressure drop at different mass fluxes are different. For stratified flow at low mass fluxes, the liquid pool at the bottom behaves more like single-phase flow than the top due to the thicker liquid film. For intermittent flow at high mass fluxes, the liquid slugs that block the tube behave more like single-phase flow than the vapor slugs, who resembles annular flow or stratified flow depending on the film thickness at the top and bottom.

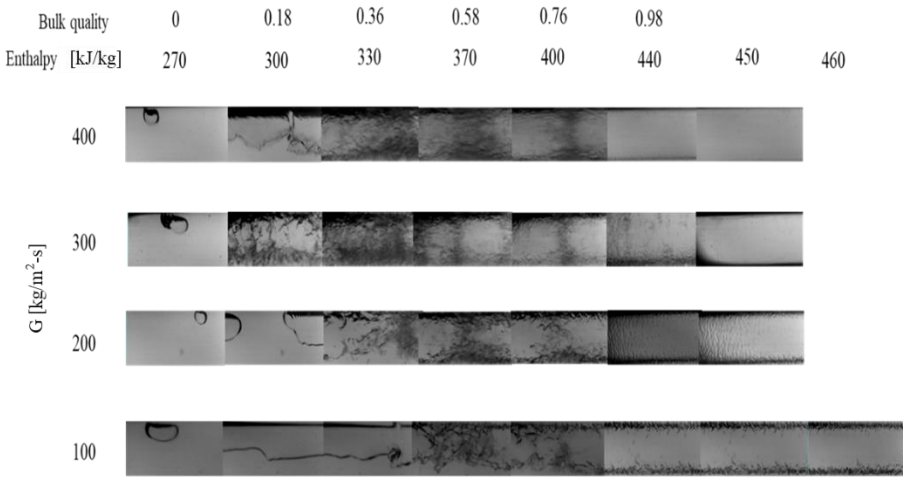


**Figure 5:** Flow visualization of R245fa during condensation at 30 ºC for four different mass fluxes

## 3.2 Effects of refrigerant properties

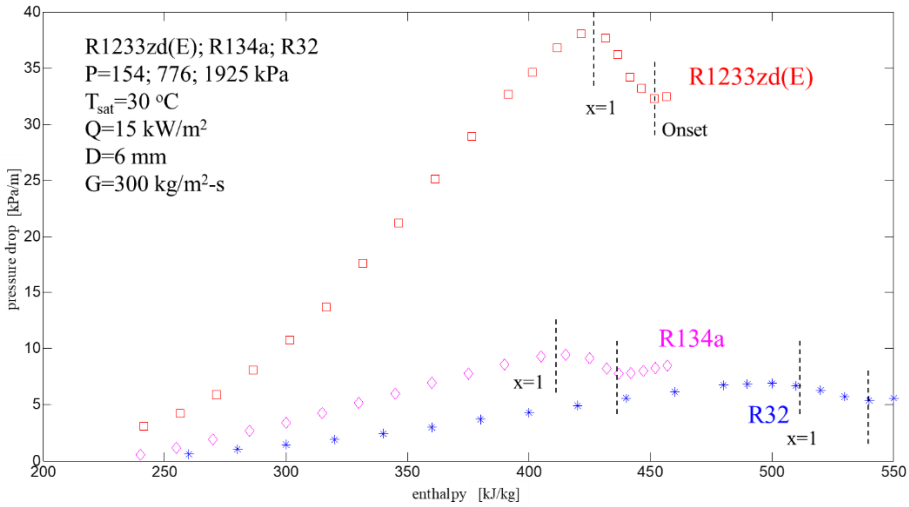


**Figure 6:** Pressure drop varies with different refrigerants.

**Table 1:** Properties of three different refrigerants.

| 30 °C | $\frac{\rho_l}{\rho_v}$ | $\sigma$ [mN/m] | $\mu_v * 10^5$ [Pa s] | $\mu_l * 10^4$ [Pa s] | $h_{fg}$ [kJ/kg] |
|---|---|---|---|---|---|
| R134a | 38.1 | 7.4 | 1.2 | 1.8 | 173 |
| R32 | 19.8 | 6.0 | 1.3 | 1.1 | 261 |
| R1233zd(E) | 51.1 | 13.9 | 1.0 | 4.4 | 186 |

In Fig. 6, pressure drops of three different refrigerants under the same working condition (except the inevitable different saturation pressure due to their different properties) is compared. The refrigerant properties are listed in Table 1. It should be noted first that the properties for R1233zd(E) might contain large error. The properties for R1233zd(E) here is for the purpose of comparison and should be used with caution.

It is obvious in Fig. 6 that R1233zd(E) has much larger pressure drop than R134a, whose pressure drop is a little larger than R32. R134a is used as baseline for comparison. For R1233zd(E), the liquid-vapor density ratio is larger than that of R134a, meaning the slip velocity is higher for R1233zd(E). The higher the velocity difference, the stronger the interaction between liquid and vapor. Hence the larger the pressure drop. Besides, the liquid viscosity of R1233zd(E) is almost 4 times of R134a, which also contributes to the higher pressure drop. The surface tension is smaller for R134a. Since the surface tension restrains wave generations, the effects from surface tension goes against the result that R134a has lower pressure drop. Obviously, the density ratio and viscosity differences between R134a and R1233zd(E) overwhelms the difference in surface tension, resulting in much higher pressure drop of R1233zd(E).

As for R32, the latent heat is much larger than that of R134a. The larger latent heat yields thinner film, which reduces wave generations, thus reduces pressure drop. The density ratio is around half for R32 compared with R134a. This means the slip velocity is smaller for R32, which also leads to lower pressure drop. The liquid viscosity is also smaller for R32. With other properties comparable in value with R134a, it is natural that R32 has a lower pressure drop than R134a.

The flow visualizations in Fig. 7 demonstrates the differences between R245fa, R134a and R32. R245fa with the larges density ratio, for example, has more vigorous waves than R32, whose density ratio is much smaller. Also, because the latent heat of R32 is much larger than the other two refrigerants, the liquid film of R32 is apparently the thinnest. The comparisons between the three refrigerants highlights the importance of waves and film thickness in predicting the pressure drop for refrigerants with different properties. When modeling these parameters, properties in Table 1 can be helpful. The comparisons in pressure drop made in this subsection provide a general sense of how those properties are connected to the pressure drop.

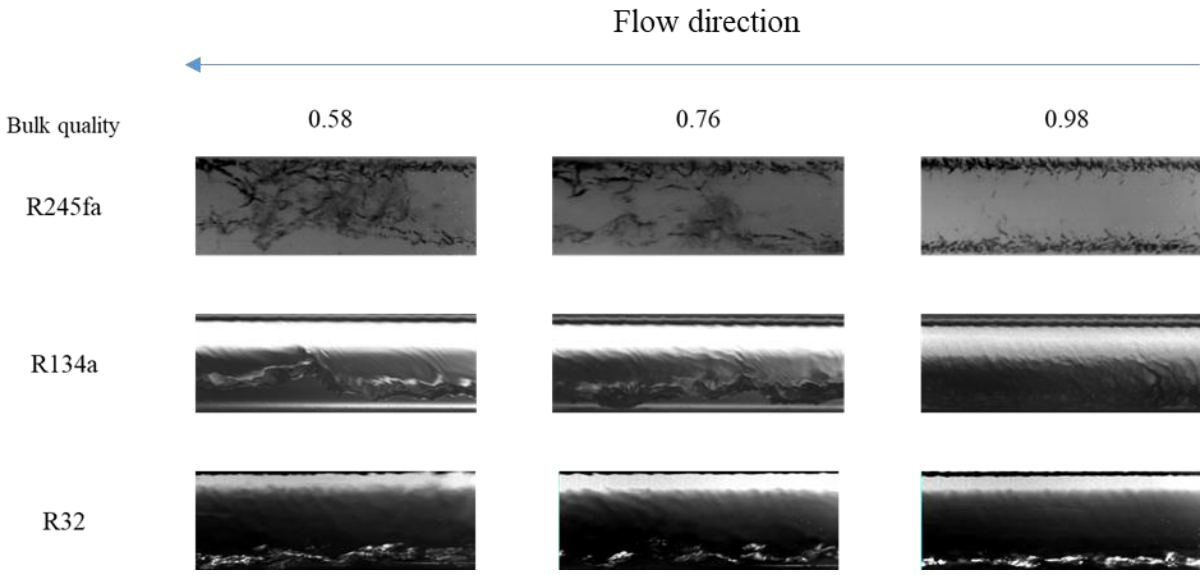


**Figure 7:** Flow visualizations of R245fa, R134a and R32 at a same mass flux of 100 kg/m$^2$-s.

### 3.3 Effects of the tube diameter

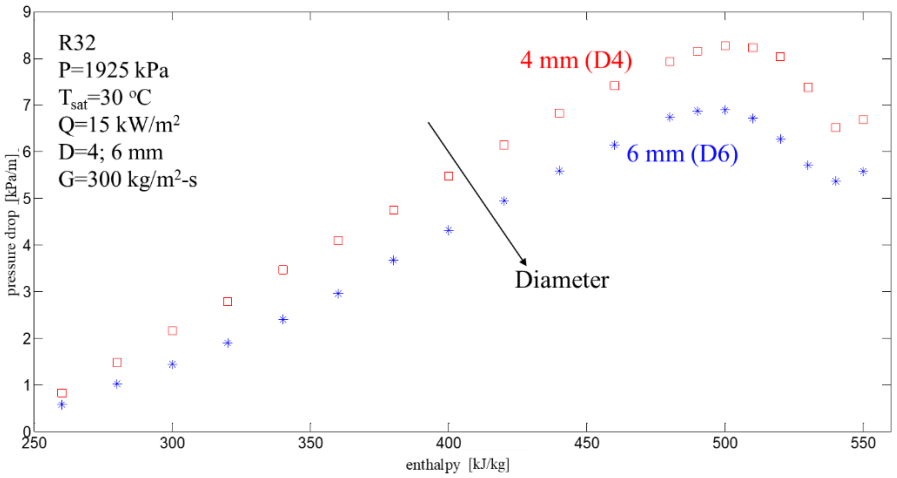


**Figure 8:** Pressure drop decreases as the tube diameter increases.

The effects of the tube diameter are straight forward just like the mass flux. Mass flux affects the pressure drop by varying velocity differences between liquid and vapor, which changes the velocity gradient. Tube diameter directly affects the velocity gradient by changing the distance between the maximum and zero (no-slip assumption at wall) velocity. Therefore, the smaller the tube, the higher the pressure drop as presented in Fig. 8. With the change from 6.1 mm to 4.0 mm, unlike mass flux and fluid properties, the flow regime is not pronouncedly different in Fig. 9. However, as the tube gets even smaller, it is reasonable to believe the capillary force will begin to play a more important role and the flow regime is very likely to be different. The general trend of pressure drop against tube diameters should be the same regardless of absolute tube size because the link between pressure drop and tube size as described above remains the same.

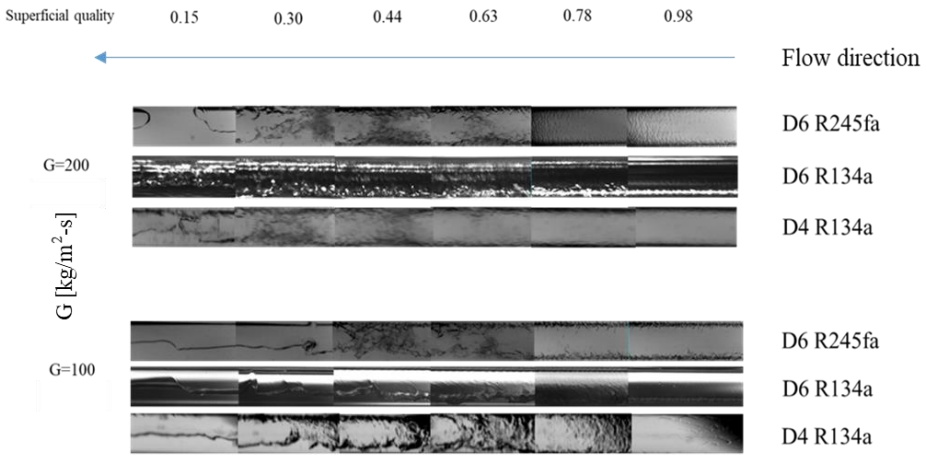


**Figure 9:** Effects of the tube diameter on flow regime is not obvious under changes from 6.1 to 4.0 mm.

### 3.4 Comparison to a "3-zone" model

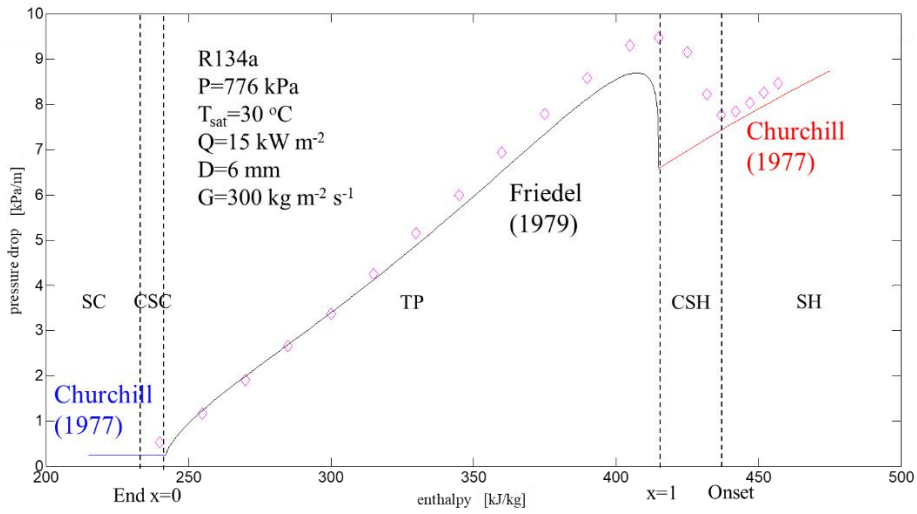


**Figure 10:** Comparison between experimental data and a "3-zone" model.

Fig. 10 compares pressure drop data with Friedel (1979) for two-phase and Churchill (1977) for single-phase flow within a conventional "3-zone" model. It should be noted that the reason Friedel and Churchill connect with each other at the bulk quality 1 and 0 is that the frictional factor used in Friedel is manually set to be determined by Churchill instead of Blasius as it usually is. Even so, the pressure drop correlation is still insufficient to represent the experimental data, especially in the CSH region. The Churchill correlation largely underpredicts the pressure drop in the CSH region because it does not include the two-phase mechanisms such as interfacial waves and slip velocity etc. Friedel correlation is developed for the two-phase flow, but it does not cover regions outside bulk quality 1 and 0. Therefore, since the "3-zone" model ignores the non-equilibrium effects, it pays the price of not capturing the two-phase mechanism in the regions where liquid film exists. By realizing that non-equilibrium matters and tracing the development of film from the onset to the end of condensation, a more realistic and accurate pressure drop model can

be built, and the authors believe it is necessary for such a model to better represent the condensation process in a condenser of a vapor-compression system.

## 4. CONCLUSIONS

Pressure drop of R134a, R32 and R1233zd(E) are measured during condensation in a horizontal round tube from superheated vapor. Mass fluxes range from 100 to 400 kg/m$^2$-s, heat fluxes change from 5 to 15 kW/m$^2$ and tube diameters of 4.0 and 6.1 mm are used. The pressure drop increases with increasing mass flux or decreasing tube diameter. Fluid properties also affect the pressure drop. The liquid to vapor density ratio dictates the velocity difference between the vapor core and the liquid film. The higher the density ratio, the higher the pressure drop. Pressure drop also increases with increasing liquid viscosity. In a fixed working condition with changing specific enthalpy, pressure drop decreases first in the SH region. After the onset of the condensation, pressure drop goes up due to the increasing waviness structure at the interface even though the flow velocity decreases. The effects of reduction in flow velocity eventually outweighs the dissipation from interfacial waves and the pressure drop decreases again at some location around bulk quality 1. A comparison between pressure drop data and a "3-zone" model with Friedel and Churchill correlation shows the defect of not considering the non-equilibrium effects. Without taking the liquid film in the CSH region into account, the model severely underpredicts the experimental data in the CSH region. A mechanistic model tracing the development of liquid film from the real onset to the end of the condensation is suggested by the authors for modeling the condensation from superheated vapor in a vapor-compression system.

## NOMENCLATURE

| | | |
|---|---|---|
| SH | Superheated | |
| CSH | Condensing superheated | |
| TP | Two-phase | |
| CSC | Condensing subcooled | |
| SC | Subcooled | |
| HTC | Heat transfer coefficient | (W/m$^2$-K) |
| *T* | Temperature | (K) |
| P | Pressure | (Pa) |
| G | Mass flux | (kg/s-m$^2$) |
| Q | Heat flux | (kW/m$^2$) |
| D | Tube diameter | (mm) |
| ρ | Density | (kg m$^{-3}$) |
| μ | Dynamic viscosity | (kg/m-s) |
| σ | Surface tension | (N/m) |
| x | Thermal dynamic quality | |

**Subscripts**

| | |
|---|---|
| r | Refrigerant |
| sat | Saturated |
| w | Water |
| i | Inlet |
| o | Outlet |

## REFERENCES

Agarwal, R., Hrnjak, P., 2015, Condensation in two phase and desuperheating zone for R1234ze(E), R134a and R32 in horizontal smooth tubes, *Int. J. Refrigeration*, vol. 50, p. 172-183.

Churchill, S.W., 1977, Friction-factor equation spans all fluid-flow regimes. *Chem. Eng*, vol. 7, p. 91–92.

Friedel, L., 1979, Improved friction pressure drop correlation for horizontal and vertical two phase flow, *3R Int*. vol. 18, p. 485–491.

Kondou, C., Hrnjak, P., 2011a, Heat rejection from R744 flow under uniform temperature cooling in a horizontal smooth tube around the critical point, *Int. J. Refrigeration*, vol. 34, no. 3, p. 719-731.

Kondou, C., Hrnjak, P., 2011b, Heat rejection in condensers close to critical point-desuperheating, condensation in superheated region and condensation of two phase fluid, *Int. Conf. Heat Trans. Fluid Mech. and Thermodynamics*, Mauritius.

Kondou, C., Hrnjak, P., 2012, Condensation from superheated vapor flow of R744 and R410A at subcritical pressures in a horizontal smooth tube, *Int. J. Heat Mass Transfer*, vol. 55, p. 2779-2791.

Meyer, M., Hrnjak, P., 2017, Flow regimes during condensation in superheated zone, *Int. J. Refrigerant*, vol. 84, p. 336-343.

Xiao, J., Hrnjak, P., 2016, Heat transfer and pressure drop of condensation from superheated vapor to subcooled liquid, *Int. J. Heat Mass Transfer*, vol. 103, p. 1327-1334.

Xiao, J., Hrnjak, P., 2017a, A new flow regime map and void fraction model based on the flow characterization of condensation, *Int. J. Heat Mass Transfer*, vol. 108, p. 443-452.

Xiao, J., Hrnjak, P., 2017b, A heat transfer model for condensation accounting for non-equilibrium effects, *Int. J. Heat Mass Transfer*, vol. 111, p. 201-210.

## ACKNOWLEDGEMENT

The authors thankfully acknowledge the support provided by the Air Conditioning and Refrigeration Center at the University of Illinois at Urbana-Champaign and technical support from Creative Thermal Solutions, Inc. (CTS).